# Delft University of Technology

# Unprotected Left-Turn Behavior Model Capturing Path Variations at Intersections

Zhao, Jing; Knoop, Victor L.; Sun, Jian; Ma, Zian; Wang, Meng

**Important note**
To cite this publication, please use the final published version (if applicable).
Please check the document version above.

# Unprotected Left-Turn Behavior Model Capturing Path Variations at Intersections

Jing Zhao<sup></sup>, Victor L. Knoop<sup></sup>, Jian Sun<sup></sup>, Zian Ma, and Meng Wang<sup></sup>, *Member, IEEE*

*Abstract*—Path dispersion (the spatial distribution of vehicular paths) is an important feature of traffic flow inside intersections and differs from traffic flow running along traffic lanes at road segment, especially under conflicting movements. The path dispersion reflects the operational features of traffic flow and is related to driving behaviour, arrival flow patterns, layout design, and the traffic control and management scheme. This study aims to improve the understanding of the overall path dispersion of unprotected left-turns and the opposing through movement. A behavioural simulation model was established to represent the overall path dispersion. Human behaviours regarding vehicle trajectory planning with and without conflicting vehicles were modelled based on optimal control and integrated into the proposed discrete event simulation framework. The descriptive power and accuracy of the proposed simulation model were validated using empirical data. The effects of the spatial size of the intersection, crossing angle, and traffic volume on the path dispersion of the left-turn and through movement were explored based on numerical experiments. The results show that the proposed simulation model can represent the path dispersion of left-turn and opposing through movement well for both the calibrated intersections and newly added intersections without model parameter recalibration with an average error of 8.92%.

*Index Terms*—Path dispersion, driving behaviors, conflicting movements, intersections.

## I. INTRODUCTION

CONFLICTS between left-turn and through movements are critical for traffic operations inside intersections, especially for intersections without a protected left-turn phase. Although the traffic rules of many countries require that left-turn vehicles yield for through vehicles, the yielding decision is subjective, and drivers must decide according to

Jing Zhao is with the Department of Traffic Engineering, University of Shanghai for Science and Technology, Shanghai 200093, China (e-mail: jing_zhao_traffic@163.com).

Victor L. Knoop is with the Department of Transport and Planning, Delft University of Technology, 2628 CN Delft, The Netherlands (e-mail: V.L.Knoop@tudelft.nl).

Jian Sun and Zian Ma are with the College of Transportation Engineering, Tongji University, Shanghai 200092, China (e-mail: sunjian@tongji.edu.cn; 14_zian@tongji.edu.cn).

Meng Wang is with the "Friedrich List" Faculty of Transport and Traffic Sciences, Technische Universität Dresden, 01069 Dresden, Germany, and also with the Department of Transport and Planning, Delft University of Technology, 2628 CN Delft, The Netherlands (e-mail: meng.wang@tu-dresden.de).

the dynamic states of interacting vehicles. Moreover, vehicles in the intersection follow a two-dimensional (2D) path. Vehicle control has two degrees of freedom: the speed and steering angle. Drivers choose their (preferred) trajectory among infinite possibilities. Even under the same yielding decision, various control strategies can be operated, including slowing down, stopping, and/or detouring. These phenomena constitute the complex path dispersion of left-turn and opposing through movements at intersections.

Existing studies on conflicting movements at intersections mainly focus on discrete interaction (yielding or crossing) decisions. The critical influencing factors of the interaction decisions, such as time gap, time-to-arrival, and conflicting distance, are mainly determined based on the restrictive assumption of a fixed conflict point [1], [2]. Microscopic vehicle movements are modelled based on lane-based models that originate in road segments, even though there are no lanes inside the intersection area. Vehicles in the microscopic simulation have to move along the (non-existing) traffic lane or move from one lane to another. Consequently, the existing commercial microscopic simulation tools assume the paths inside the intersections are fixed because the traffic lanes should be pre-determined before simulation. Some models, such as the cellular automata model [3], [4], [5], can make a more detailed description with a smaller cell size, but vehicles must still run along the cells.

In practice, simulation models are helpful for evaluating the performance of intersection designs. However, vehicles will always run exactly along the path set by modellers, and hence there is no path dispersion. This situation is unrealistic because no matter how poor the intersection design is, vehicles always run smoothly, and the conflicting movement flow pairs always have fixed conflict points.

This study establishes a simulation model that describes the paths of left-turning vehicles under the unprotected left-turn phase inside intersections. The proposed model is based on driver behavioural analysis. Contrary to the widely-used simulation models, such as Vissim, Paramics, and Aimsun, the proposed simulation model can endogenously describe the paths of interacting vehicles rather than setting them as simulation inputs. The overall path dispersion thereof is an output, which is a more realistic description of the traffic flow inside intersections. The model, in turn, can be used to assess designs. Indeed, the designs should give the drivers reasonable guidance at intersections. For different designs, we can obtain their path dispersion indicators based on the simulation model. Then, the effectiveness of guiding traffic

flow can be compared. Therefore, the proposed simulation model can assess the effectiveness of a particular design. The path dispersion description is useful for conditions of highly heterogeneous traffic with weak lane discipline, especially in developing countries, such as China and India [6], [7], [8], [9]. We also realise the complexity of the path dispersion, which may be affected by geometric conditions, signal control conditions, traffic conditions, and driver characteristics. The proposed model can be a starting point and extended with more real-world considerations in future studies.

The paper is organised as follows. Section II reviews the relevant studies and motivates the contribution of our proposal. Section III conducts an empirical analysis on the path dispersions of the unprotected left-turn and opposing through movement. Two indicators that can analyse the path dispersion quantitatively are introduced. Section IV describes the formulation of the trajectory planning model, parameter calibration, and simulation framework. Section V validates the accuracy of the proposed model based on comparative analysis using empirical data. Section VI discusses the sensitivity of influencing factors, and the study is concluded in Section VII.

## II. Literature Review of Conflicting Movements at Intersections

The relevant studies on the path dispersion of conflicting movements at intersections mainly contain three aspects: gap acceptance, microscopic traffic flow models, and vehicle trajectory models and analysis inside intersections.

Studies of gap acceptance focus on whether a gap will be accepted and mechanisms influencing the acceptance based on discrete decision models. Numerous empirical and driving simulator-based studies show that the vehicular yielding/crossing behaviour is an inherently complex process affected by various factors, including geometric design, traffic conditions, vehicle features, and driver characteristics. (1) For geometric designs, Yan and Radwan [10] used field data to show that drivers' restricted sight distance increases the critical gap and follow-up time. Devarasetty et al. [11] developed a binary logit model to predict the gap acceptance probability considering the gap duration, total wait time, time to turn, distance to the next downstream signal, and median type. (2) For traffic conditions, Liu et al. used empirical data to identify the decisive moment for crossing and merging behaviour based on classification tree analysis [12], [13]. The influencing factors related to the speed and distance were investigated. Patil and Pawar [14] used field data to analyse the critical temporal and spatial gap without explicit priority. Hutton et al. [15] modelled the critical gap as a function of the left-turn lane offset based on comprehensive naturalistic driving data. (3) For vehicle features, Robbins et al. [16] compared the reaction of drivers when facing the conflict with cars and motorcycles based on driving simulator experiments. The results show that significantly smaller (riskier) gaps in front of motorcycles were accepted than in front of cars. (4) For driver characteristics. Yan et al. [17] explored the effects of traffic speed and driver age and gender based on driving simulator experiments. Bärgman et al. [18] proposed that

two boundaries, namely comfort- and dread-zone boundaries, are needed to predict the behaviour of the left-turn crossing. Drivers do not cross without extra motives for the comfort-zone boundary, while drivers do not cross even with extra motives for the dread-zone boundary. Tang et al. [19] proposed a gap acceptance model for left-turn considering the trade-off between the perceived risk and time-saving benefit. Liu et al. [20] established a crossing behaviour model based on an analysis of the interaction among the drivers' risk perception, acceptable risk level perception, and vehicle motion state. Mao et al. [21] used the logistic regression model to obtain critical gaps considering the cognitive behaviour of drivers, and estimated the safety of the gap. Paschalidis et al. [22] used driving simulator data to investigate the effect of driver stress levels on their gap acceptance at an intersection. Gao et al. considered driver aggressiveness and analysed illegal permissive left-turning movement conditions [23], [24]. Li et al. [25] analysed the effect of mobile phone use on the gap acceptance manoeuvre at intersections. These yielding/crossing prediction models are discrete decision models. In these studies, to calculate the gap and influencing factors, the researchers assumed the trajectories of the conflicting movements to be pre-determined and neglected path dispersion. The shortcomings of this assumption have been pointed out, especially in the non-lane-based traffic environment [26].

For microscopic traffic flow, numerous studies explored the interaction between vehicles and their effects on traffic flow. Traffic management and signal control are the influencing factors considered in the existing studies. Based on the Newell [27] car-following model, Ahn et al. [28] analysed the temporal and spatial characteristics of trajectories under signal timing. Considering various signal control scenarios, Sasaki and Nagatani [29] analysed the traffic flow variation under the simple synchronised, green wave, and random switching signal strategies. The traffic phenomena caused by the signal control, including clustering, dissipating, and wave propagation, were explored by Tang et al. [30]. The effect of the green signal countdown device, which is widely used in China, on these phenomena was further discussed [31], [32]. To achieve a more realistic representation of driving behaviour, human-factors were also considered in modelling [33]. The effects of many advanced traffic managements on the microscopic traffic flow were also explored based on the microscopic traffic flow model, including the speed guidance system [34], [35] and the automation and communication technology [36], [37], [38]. Although much is known on the vehicle behaviour and its corresponding effects on traffic flow at intersections, the traditional microscopic traffic flow is lane-based. Based on these traditional car-following and lane-changing models, the existing commercial microscopic simulation models are also lane-based. Some microscopic traffic models were generalised to consider vehicles' 2D movement under the weak discipline of lane-based driving conditions. At road segments, Gunay [39] developed a car-following model with the considering the discomfort caused by lateral friction between vehicles, which is formulated as a function of the off-centre effects. Jin et al. [40] extended the full velocity difference

car following model by considering the effects of the lane width and lateral separation between vehicles. Kanagaraj and Treiber [41] developed a 2D multi-particle model for mixed motorised and non-motorised traffic flow, where longitudinal and lateral dynamics are connected.

Inside intersections, vehicle movements become more complex. Previous studies focused on vehicular trajectory modelling and influencing factor analysis of conflicting movements. The methods mainly include the following four groups:

(1) Extending the car-following model. Delpiano et al. [42] proposed a 2D microscopic traffic model by modelling the multi-directional collision avoidance behaviour of drivers as a 2D repulsive force between vehicles. Xie et al. [43] proposed a 2D car-following model to describe the mixed traffic flow at unsignalised intersections. The interactions between a vehicle and other motorised/non-motorised vehicles were considered.

(2) Statistic and machine learning-based model. Zhang et al. [44] developed a probability prediction model based on binary logistic analysis to explore various factors affecting the probability of left-turn paths. Azadani and Boukerche [45] introduced a novel deep learning-based methodology to anticipate vehicle paths at unsignalised intersections. Choi et al. [46] explored the relationship between crashes and turning paths at intersections. It found that ageing drivers exhibit greater and more inconsistent offsets during turning movements than younger drivers. Zhang et al. [47] proposed a long short-term memory-based (LSTM-based) vehicle motion prediction model that combines intention and trajectory predictions.

(3) Social force model. Ma et al. [48] used the social force model to generate 2D vehicle movements. The trajectory is obtained by the integrated effect of forces, such as the self-driven, repulsive, and attractive forces [49], [50], [51]. They further proposed a three-layered plan-decision-action framework to obtain acceleration and angular velocity in the turning process [52].

(4) Optimal control model. At the beginning, researchers modelled the paths inside intersections [53], [54], [55] and roundabouts [56] using a combination of straight lines and parametric curves considering the intersection geometry, vehicle type, and speed. Recently, Bichiou and Rakha [57] developed a 2D trajectory planning model for autonomous vehicles considering the collision avoidance constraints and detailed vehicle motion. The algorithm was further simplified for real-time control [58]. For human drivers, Zhao et al. [59] proposed a 2D vehicle movement model with the consideration of drivers' efficiency and comfort preferences. Dias et al. [60] explored the applicability of the minimum-jerk principle to model and simulated free-flow trajectories of turning vehicles. Ziegler et al. [61] modelled the human-driven trajectories of vehicles by using a time-discrete kinematic bicycle model with the vehicle's acceleration and steering rate as inputs.

The existing trajectory models for intersections mainly focus on controlling individual vehicles. The overall path dispersion is neglected in the existing traffic flow analysis.

In summary, the overall path variation analysis is ignored in current gap acceptance behaviour models, traditional traffic flow models, and vehicle trajectory planning studies. The contribution of this study lies in the development of a behaviour-based simulation model that describes the *overall* path dispersion for the unprotected left-turn and opposing through movements at intersections. The proposed model integrates tactical-level decisions and operational-level vehicle trajectories and can endogenously describe the paths of interacting vehicles rather than setting them as simulation inputs. Empirical data are used to verify the plausibility and effectiveness of the proposed model. The proposed simulation model provides insights on the *overall* operating condition of the conflicting movements inside intersections.

## III. EMPIRICS

In this section, the real-world path dispersions of the unprotected left-turn and opposing through movement are illustrated.

### A. Data Collection

The real vehicle trajectories in nine intersections with the permitted left-turn phase are collected by drones. The coordinates of left-turn and through vehicles are collected in 24 frames per second. The selected intersections should contain directions with the unprotected left-turn phase. Moreover, various types of intersection and traffic lane numbers of approach should be covered. The basic information of surveyed intersections and recording view are shown in Table I. The nine surveyed intersections contain six cross intersections, two T-shaped intersections, and a Y-shaped intersection. The traffic lane number of the approach contains one, two, and three lanes.

### B. Path Dispersion Analyses Method

To analyse the path dispersion quantitatively, we used the following indicators: (1) the frequency of path coverage (FPC) at each lattice, and (2) the standard deviation (SD) of the paths. The former can be regarded as an overall description of the path dispersion in space, while the latter can quantitatively describe the statistical dispersion of the paths.
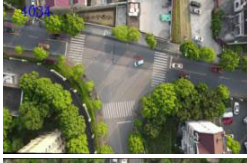
The FPC can intuitively show the path dispersion. As illustrated in Fig. 1, we generate a mesh inside the intersection. In this study, the mesh is generated with a resolution of 1 m in the longitudinal and lateral directions. The FPC at each lattice can be calculated by Eq. (1).

$$FPC_l = N_l/N, \quad \forall l \in L \tag{1}$$

where, $FPC_l$ is the frequency of path coverage at lattice $l$; $N_l$ is the number of vehicles traversing at lattice $l$, veh; $N$ is the total number of vehicles in the specific movement direction, veh; $L$ is the set of lattices.

The SD is a measure of dispersion in statistics and is the extent to which a distribution is stretched or squeezed. In this study, the SD of the paths represents the outcome of the path dispersion, which can be calculated using Eq. (2). For a set movement paths, we can fit and get a standard path in the middle of the path set. Then, we can calculate the Euclideanandistance between the points on a path and the standard path, $d_{mp}$. Each Euclidean distance is then squared,

TABLE I
SURVEYED INTERSECTIONS

| Intersection | Recording view | Collected vehicles | |
|---|---|---|---|
| | | Left-turn | Through |
| No. 1: Yangtai Road - Zhentai Road | | 66 | 107 |
| No. 2: Youyi Road – Tieli Road | | 22 | 41 |
| No. 3: Cangyi Road – Yuansheng Road | | 18 | 78 |
| No. 4: Zuchongzhi Road – Gaosi Road | | 18 | 32 |
| No. 5: Taolin Road – Linshan Road | | 16 | 26 |
| No. 6: Gaokezhong Road - Zhangdong Road | | 40 | 130 |
| No. 7: Pingdu Road - Jinyang Road | | 14 | 39 |
| No. 8: Tangxing Road - Tangzhen Road | | 25 | 22 |
| No. 9: Jiaodong Road - Mouping Road | | 21 | 18 |

and the results are summed. The result is then divided by the number of path points of the left-turn and opposing through movements; this is the variance. The SD can then be calculated
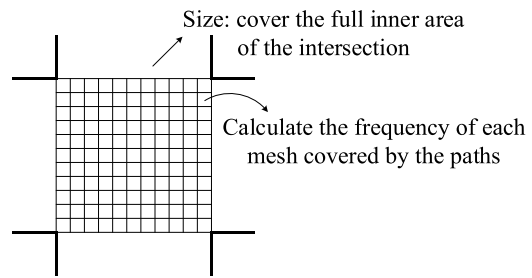


Fig. 1. Mesh inside the intersection.
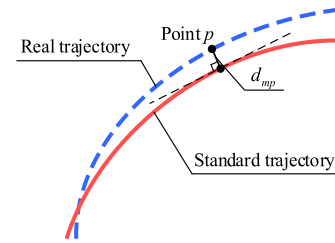


Fig. 2. Concept of $d_{mp}$.
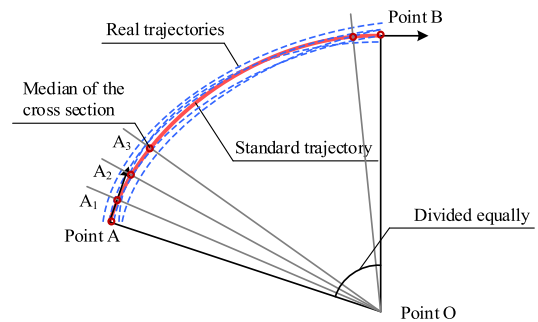


Fig. 3. Creation of the standard trajectory.

as the square root of variance.

$$SD = \sqrt{\frac{1}{\sum_{m=1}^{2} P_m} \sum_{m=1}^{2} \sum_{p=1}^{P_m} d_{mp}^2} \qquad (2)$$

where, $SD$ is the standard deviation of paths, m, which indicates the overall path dispersion; $m$ represents the movement, $m = 1$ and 2 for left-turn and through movement, respectively; $d_{mp}$ is the Euclidean distance between the point $p$ on a path and the standard path for movement $m$, m, as shown in Fig. 2; $P_m$ is the number of path points for movement $m$.

We use the following method to create the standard movement trajectory. For any movement, we have real paths from empirical data. For left-turn, first, the middle of start and terminal points can be obtained, as points A and B shown in Fig. 3. The average heading angle of start points and terminal points can also be obtained. Second, point O in Fig. 3 can be obtained, which is the cross point of the two lines perpendicular to points A and B. Third, the rays, which divide the angle into $N$ equal parts, can be drawn. In this paper, $N$ is set to be 50. Fourth, the median point of each cross-section is found. Finally, we get the standard trajectory by connecting these median points (A, $A_1$, $A_2$, $A_3$, . . . , B). For

through movement, since the heading angles of the start and terminal points are similar, the parallel lines are used instead.

### C. Path Dispersion Results

The FPC and SD values of the empirical data are illustrated in Table IV in Appendix A and Table VI in Appendix B, respectively. The data intuitively shows that the paths are dispersed, which is related to the driving behaviour, arrival flow pattern, layout design, and traffic control and management scheme. The mean of the SD is 1.25 m. To represent the path dispersion, we establish a simulation model in the next section.

## IV. MODEL ESTABLISHMENT

This section establishes a simulation model to estimate the path dispersion of two conflicting movements at signalised intersections. Model formulations in different traffic situations are first introduced. Then, the parameters that reflect driving behaviour are calibrated. They are integrated into a simulation framework to represent the path dispersion of two conflicting movements.

### A. Model Formulations in Different Traffic Situations

The movement decisions of vehicles in the simulation model contain two levels: tactical-level decisions and operational-level vehicle trajectories. At the tactical level, we decide whether the trajectory of a vehicle must be re-planned, while the trajectories are planned at the operational level.

Two types of trajectories are defined for tactical-level decisions, namely the temporary trajectory and fixed trajectory. The temporary trajectory means that vehicle's trajectory may need to be re-planned, for example, the arrival of a new conflicting vehicle. The fixed trajectory means that the trajectory of the vehicle will not be re-planned. At the tactical level, a vehicle can be given a fixed trajectory when it is the first vehicle crossing the conflict point. This situation based on the understanding that even when a new conflicting vehicle arrives, it also should yield as the front vehicle. Moreover, as time goes by, the temporary trajectory is fixed if no new conflicting vehicles arrive.

At the operational level, a new vehicle can have three possible conditions when it arrives at the analysis area: (1) there are no other vehicles in the analysis area, (2) there are vehicles at the analysis area but no vehicles of conflicting movement with temporary trajectories, and (3) there are vehicles of conflicting movement with temporary trajectories.

*1) Condition 1: No Other Vehicles in the Analysis Area:* When there are no other vehicles in the analysis area, the newly arriving vehicle becomes the only vehicle that should be considered. We can use the 2D vehicular movement model to describe the trajectory of one vehicle.

The original model proposed by Zhao et al. [59] used the travelled distance as the main independent variable. However, we need to update the states of the vehicles according to the simulation time. A time-domain model is more convenient than a distance-domain model to synchronise all the vehicles in

the simulation. Therefore, the one vehicle trajectory planning problem from the initial state to the terminal state can be formulated as following equations using Eq. (3) as the objection function and Eqs. (4) – (6) as constraints. The constraints of Eq. (4) – (6) restrict the vehicle's running speed, curvature, and acceleration. The vehicle motion dynamics and model's control variables are specified in Eqs. (7) and (8), respectively. The two control variables, the acceleration and curvature, can be regarded as the control of the throttle/brake pedals and the steering wheel of a human driver. The running cost $L_i$ in the objection function (1) reflects the different cost aspects considered by the drivers during driving, including the travel time, turning, and acceleration costs, as shown in Eq. (9).

$$\min_{\mathbf{U}_i} C\left(\mathbf{X}_i, \mathbf{U}_i\right) = \min_{\mathbf{U}_i} \int_0^{t_{fi}} L_i\left(t, \mathbf{X}_i, \mathbf{U}_i\right) \mathrm{d}t \qquad (3)$$

where, $\mathbf{X}_i(t)$ is the state vector of vehicle $i$ at time $t$; $\mathbf{U}_i(t)$ is the control vector of vehicle $i$ at time $t$, which is defined in Eq. (8); $t_{fi}$ is the time spent from the initial to the terminal state of vehicle $i$, in s; $L_i$ is the running cost of vehicle $i$ at the time $t$.

$$0 \leq v_i \leq v_{\max} \qquad (4)$$
$$-1/r_{\min} \leq \kappa_i \leq 1/r_{\min} \qquad (5)$$
$$a_{i\min} \leq a_i \leq a_{i\max} \qquad (6)$$

where, $v_{\max}$ is the maximum velocity, m/s. Since the design speed of urban streets is normally no more than 16.67 m/s (60 km/h) [62], the maximum velocity limitation is set to be 20 m/s [63] considering the temporal speeding of vehicles. $r_{\min}$ is the minimum turning radius, m, which is set to be 5 m according to the specification of urban road design engineering [62]. $a_{\min}$ and $a_{\max}$ are the minimum and maximum acceleration, respectively, m/s². The minimum acceleration is set to be -5 m/s² as in many studies [57], [64]. The maximum acceleration is more complex. A possible value of 5 m/s² is assumed according to previous studies [57].

$$\frac{\mathrm{d}}{\mathrm{d}t}\mathbf{X}_i(t) = \frac{\mathrm{d}}{\mathrm{d}t} \begin{bmatrix} x_i(t) \\ y_i(t) \\ \theta_i(t) \\ v_i(t) \end{bmatrix} = \begin{bmatrix} v_i(t)\cos\theta_i(t) \\ v_i(t)\sin\theta_i(t) \\ v_i(t)\kappa_i(t) \\ a_i(t) \end{bmatrix},$$
$$\text{with } \mathbf{X}_i(0) = \mathbf{X}_{0i} \text{ and } \mathbf{X}_i(t_{fi}) = \mathbf{X}_{fi} \qquad (7)$$

where, $x_i(t)$ and $y_i(t)$ are the plane coordinate of vehicle $i$ at time $t$, s; $\theta_i(t)$ is the heading angle of vehicle $i$ at time $t$, rad; $v_i(t)$ is the velocity of vehicle $i$ at time $t$, m/s; $\kappa_i(t)$ is the curvature (reciprocal of the turning radius) of the trajectory of vehicle $i$ at time $t$, rad/m; $a_i(t)$ is the longitudinal acceleration of vehicle $i$ at time $t$, m/s²; $\mathbf{X}_{0i}$ is the initial state of vehicle $i$; $\mathbf{X}_{fi}$ is the terminal state of vehicle $i$.

$$\mathbf{U}_i(t) = \begin{bmatrix} \kappa_i(t) \\ a_i(t) \end{bmatrix} \qquad (8)$$

$$L_i = \sum_j \beta_{ji} L_{ji} = \beta_{1i} + \frac{\beta_{2i}}{2}a_{ci}^2 + \frac{\beta_{3i}}{2}a_i^2 \qquad (9)$$

where, $L_{ji}$ is the running cost $j$ of vehicle $i$; $\beta_{ji}$ is the weight of the running cost $j$ of vehicle $i$, which reflects the driving

TABLE II
DESCRIPTIVE STATISTICS OF THE CALIBRATED PARAMETERS

| Parameter | ` Movement | Mean | Standard deviation |
|---|---|---|---|
| $\beta_2$ | Left-turn | 0.206 s$^4$/m$^2$ | 0.187 |
| $\beta_3$ | Left-turn | 0.232 s$^4$/m$^2$ | 0.199 |
| $\beta_4$ | Left-turn | 0.563 s$^2$/m | 0.222 |
| $\beta_2$ | Through | 0.220 s$^4$/m$^2$ | 0.216 |
| $\beta_3$ | Through | 0.240 s$^4$/m$^2$ | 0.240 |
| $\beta_4$ | Through | 0.313 s$^2$/m | 0.143 |

TABLE III
SIGNIFICANCE TEST OF LEFT-TURN AND THROUGH VEHICLES

| Parameter | t | df | Sig. (2-tailed) | Mean difference | Std. error difference | 95% confidence interval of the difference | |
|---|---|---|---|---|---|---|---|
| | | | | | | Lower | Upper |
| $\beta_2$ | -0.558 | 248 | 0.578 | -0.014 | 0.026 | -0.065 | 0.036 |
| $\beta_3$ | -0.259 | 248 | 0.796 | -0.007 | 0.028 | -0.062 | 0.048 |
| $\beta_4$ | -10.559 | 211.8 | 0.000 | -0.250 | 0.024 | -0.296 | -0.203 |

behaviour of human drivers; $a_{ci}$ is the lateral acceleration, in m/s$^2$, which can be determined by Eq. (10).

$$a_{ci} = \kappa_i v_i^2 \tag{10}$$

*2) Condition 2: Other Vehicles Present but No Vehicles of Conflicting Movement With Temporary Trajectories:* In this condition, since there are no conflicting vehicles or the conflicting vehicles have fixed trajectories, we can use the one-vehicle trajectory planning model mentioned above by considering the effect of all other vehicles. Therefore, Eq. (9) should be replaced by Eq. (11), while keeping Eqs. (3) − (8) and (10) the same. The added $v_{rib}^2 e^{-D_{ib}}$ term is a function of the radial velocity and distance, which can reflect the effect from all other vehicles for safety considerations.

$$L_i = \sum_j \beta_{ji} L_{ji} = \beta_{1i} + \frac{\beta_{2i}}{2} a_{ci}^2 + \frac{\beta_{3i}}{2} a_i^2 + \beta_{4i} v_{rib}^2 e^{-D_{ib}} \tag{11}$$

where, $v_{rib}$ is the radial velocity of the interacting vehicle $b$ with respect to the target vehicle $i$, m/s, which can be calculated using Eq. (12); $D_{ib}$ is the distance between two vehicles, m, as shown in Eq. (13).

$$v_{rib} = \begin{cases} v_i cos\varphi_{ib} + v_b cos\gamma_{ib}, & v_i cos\varphi_{ib} + v_b cos\gamma_{ib} \geq 0 \\ 0, & v_i cos\varphi_{ib} + v_b cos\gamma_{ib} < 0 \end{cases} \tag{12}$$

where, $v_b$ are the velocities of the interacting vehicle $b$, in m/s; $\varphi_{ib}$ is the angle between the direction from the target vehicle $i$ to the interacting vehicle $b$ and direction of the target vehicle's velocity, in rad; $\gamma_{ib}$ is the angle between the direction from the interacting vehicle $b$ to the target vehicle $i$ and direction of the interacting vehicle's velocity, in rad.

$$D_{ib} = \sqrt{(x_i - x_b)^2 + (y_i - y_b)^2} \tag{13}$$

*3) Condition 3: Existing Vehicles of Conflicting Movement With Temporary Trajectories:* With vehicles of conflicting movement with temporary trajectories, the trajectories of the target (newly arrived) vehicle and the vehicles of conflicting movement with temporary trajectories should be jointly planned. Thus, the objective function (3) of the trajectory planning should be replaced by Eq. (14) to contain the costs of all these vehicles while keeping Eqs. (4) − (8) and
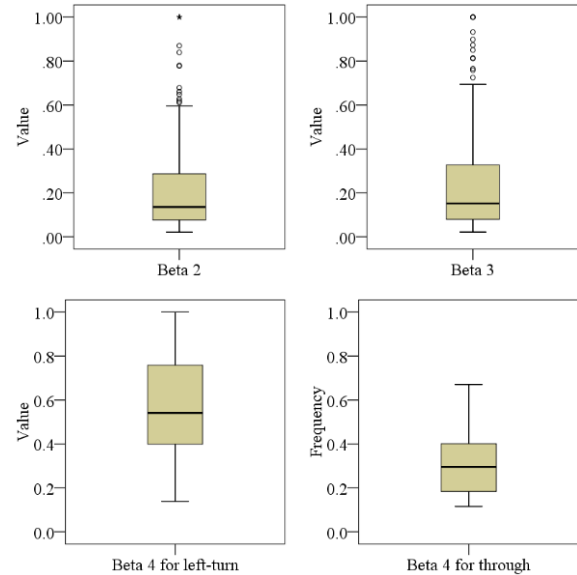


Fig. 4.   Box-plot of the calibrated parameters.

(10) − (13) the same. Then, the crossing order and trajectories of the conflicting vehicles can be obtained simultaneously. The vehicle that crosses first can get a fixed trajectory, which is used in tactical-level decisions.

$$\min_{\mathbf{U}} \left( \sum_i \int_0^{t_{fi}} L_i dt, \forall i \in I \right) \tag{14}$$

where, $\mathbf{U}$ is the set of $\mathbf{U}_i$; $I$ is the set of considered vehicles, including the target (newly arrived) vehicle and vehicles of conflicting movement with temporary trajectories.

Therefore, in the proposed model, the crossing order of conflicting movement is used to distinguish temporary and fixed trajectories. Then, the vehicle crossing the conflict point first is given the fixed trajectory. However, the positions of conflict points are not fixed nor determined as a priori. Each conflict point is endogenously generated by our model and the position varies depending on the interaction between conflicting vehicle pairs.

### B. Model Calibration to Reflect Various Driving Behaviour

The driving behaviour can be reflected by the parameters ($\beta_1$, $\beta_2$, $\beta_3$, and $\beta_4$) in the model. The four parameters, $\beta_1$, $\beta_2$, $\beta_3$, and $\beta_4$, reflect the drivers' concerns on the travel time, lateral acceleration, longitudinal acceleration, and safety,

Fig. 5.   Simulation procedure.
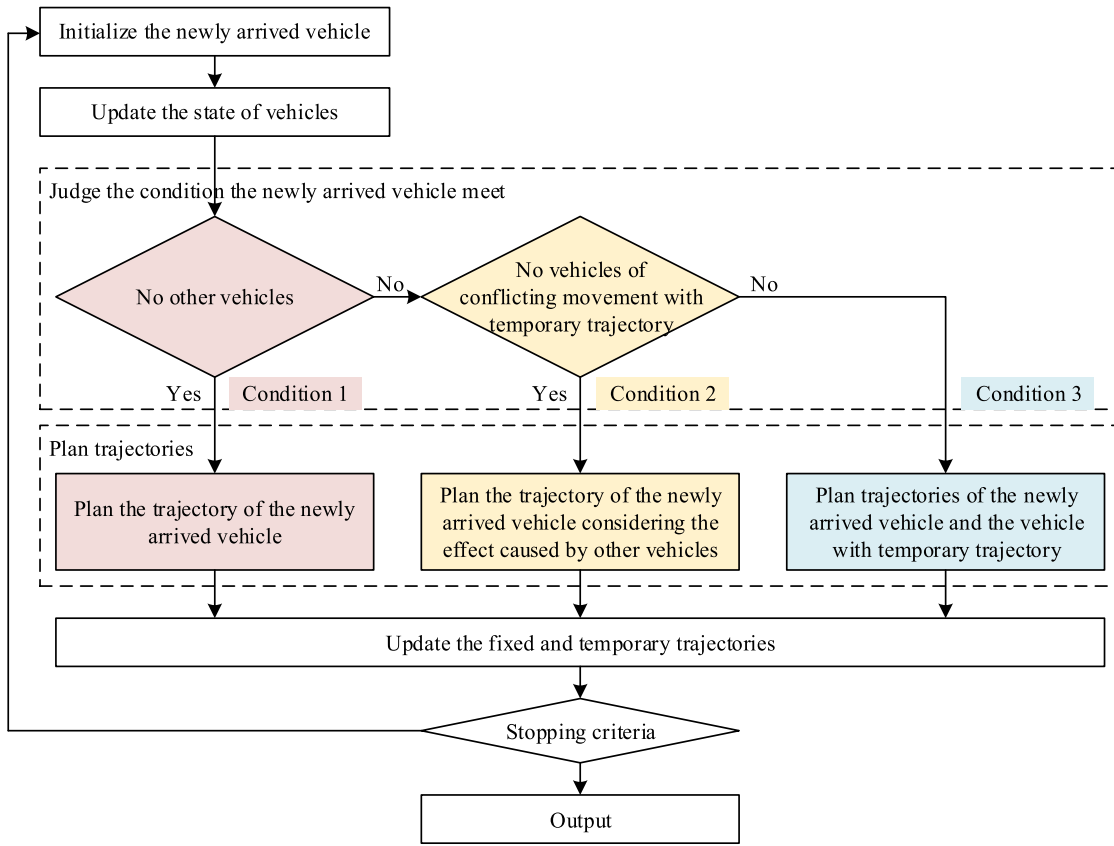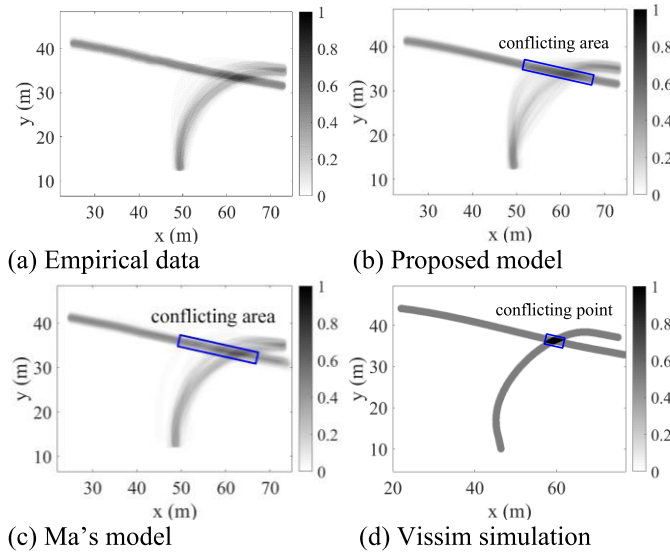


(a) Empirical data

(b) Proposed model

(c) Ma's model

(d) Vissim simulation

Fig. 6.   FPC comparison (No. 8 intersection).

respectively. Since the degree of importance is relative, we can set $\beta_1$ to 1 for convenience. In this section, we use the empirical data to calibrate the other parameters ($\beta_2$, $\beta_3$, and $\beta_4$) to ensure the model's reality.

In the nine surveyed intersections shown in Table I, the data from the first five intersections (No. 1-5) are used for parameter calibration. The data from the other four intersections

(No. 6-9) are used only for model validation in Section V to check the performance of the model in new intersections (i.e., not being used in the calibration).

*1) Parameter Calibration:* The sequential quadratic programming (SQP) method [65] was used to obtain the optimal parameters for each conflicting vehicle pair that minimise the root-mean-square error (RMSE) of the discrepancy between the modelled and collected trajectories, as shown in Eq. (15).

$$RMSE = \sqrt{\sum_{t=1}^{n} \left[ \left( x_t^m - x_t^c \right)^2 + \left( y_t^m - y_t^c \right)^2 \right] / n} \quad (15)$$

where, $\left( x_t^m, y_t^m \right)$ and $\left( x_t^c, y_t^c \right)$ are the coordinates of the modelled and collected trajectories at time $t$, respectively m.

The descriptive statistics of the calibrated parameters are shown in Table II. The result of the independent-samples T-test (Table III) shows that the differences in $\beta_2$ and $\beta_3$ between left-turn and through vehicles are not significant ($p > 0.05$), while the difference of $\beta_4$ between left-turn and through vehicles is significant ($p < 0.05$). Therefore, for $\beta_2$ and $\beta_3$, we merge the data from left-turn and through vehicles. For $\beta_4$, they are divided into two data sets.

*2) Parameter Sampling:* The box-plot of the calibrated parameters is shown in Fig. 4. Compared to the through vehicles, the left-turn vehicles care more about safety and most (25% − 75% percentiles) of the $\beta_2$ and $\beta_3$ values for left-turn and through vehicles are in the range of [0.07, 0.28] and [0.08, 0.30], respectively. For $\beta_4$, most (25% - 75% percentiles) values for left-turn vehicles and through movement are [0.40,
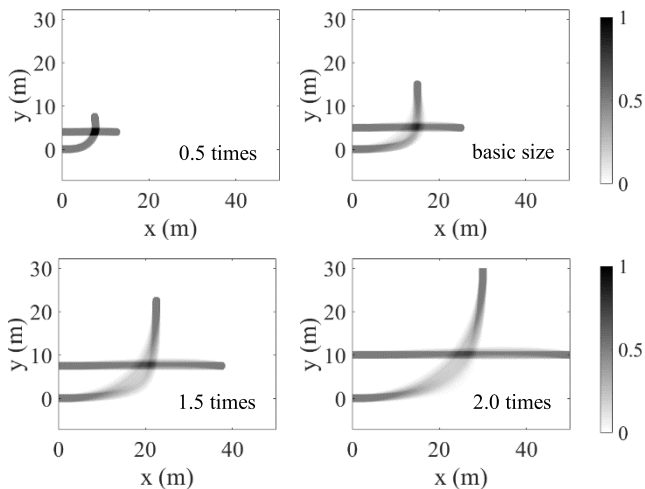
(a) FPC under different spatial sizes of the intersection
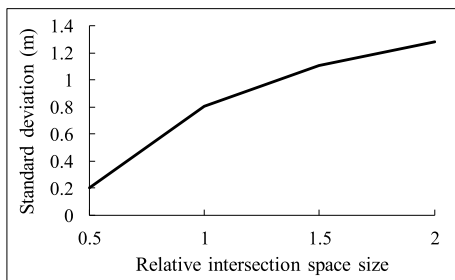


(b) Change of SD against the size of the intersection

Fig. 7.   Impact of the intersection's spatial size.



(a) FPC under different crossing angles



(b) Change of SD against the crossing angle

Fig. 8.   Impact of the crossing angle.

0.77] and [0.18, 0.40], respectively. Therefore, parameters are selected randomly from these ranges in the hereafter analysis, reflecting the heterogeneity of driving behaviour.
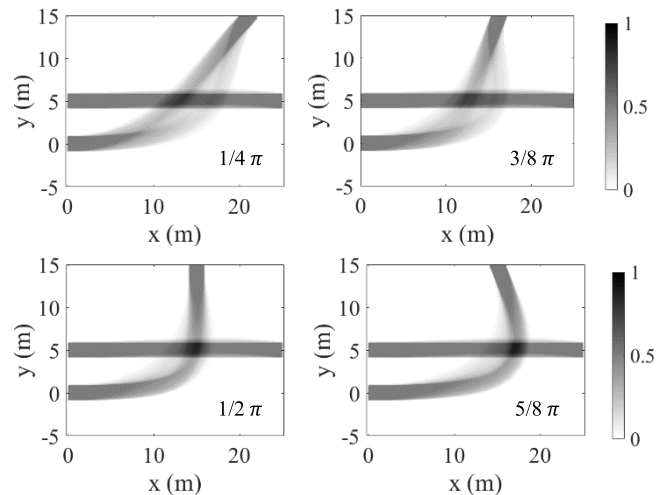
## C. Simulation Procedure

A discrete event simulation framework is used, as shown in Fig. 5. When a new vehicle arrives, the process of the contains six steps. At the end of the analysis period, the path dispersion can be estimated.
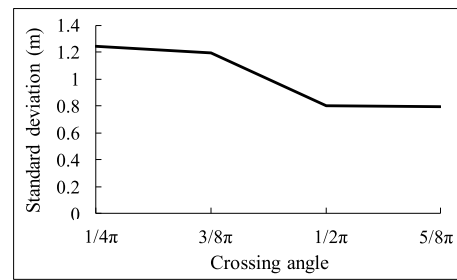
Step 1: Initialise the newly arriving vehicle. When a new vehicle arrives, the parameters related to the vehicle are initialised. They include the arrival time ($T_i$), movement ($M_i$), initial state ($\mathbf{X_{0i}}$), terminal state ($\mathbf{X_{fi}}$), maximum velocity ($v_{\max}$), minimum turning radius ($r_{\min}$), and minimum and maximum accelerations ($a_{\min}$, $a_{\max}$).

Step 2: Update the states of all the vehicles in the analysis area. The current vehicular states are updated according to the planned trajectories, which contain four aspects. First, the temporary trajectories from the arrival time of the last vehicle to the current time should be fixed. Second, if a vehicle $i'$ has arrived at the terminal state, it should be removed from the analysis system, as shown in Eq. (16). Third, the number of vehicles and vehicles with the temporary trajectory in the system can be updated by Eqs. (17) – (19). Fourth, the position, heading angle, and velocity of each vehicle in the system should be updated, as shown in Eq. (20).

$$S_i = 0, \quad \forall T_i + t_{fi} \leq T \tag{16}$$

where, $S_i$ is a binary parameter indicating whether vehicle $i$ is in the system, 1-yes and 0-no; $T_i$ is the arrival time of vehicle $i$; $T$ is the current time.

$$N = \sum_i S_i \tag{17}$$

where, $N$ is the number of vehicles in the system.

$$N_1 = \sum_i S_i (1 - F_i) (2 - M_i) \tag{18}$$

$$N_2 = \sum_i S_i (1 - F_i) (M_i - 1) \tag{19}$$

where, $N_1$ and $N_2$ are the number of left-turn and through vehicles with temporary trajectories in the system, respectively; $F_i$ is a binary parameter indicating whether vehicle $i$ has fixed trajectory, 1-yes and 0-no; $M_i$ indicates the movement of vehicle $i$, 1-left-turn and 2-through movement.

$$\begin{bmatrix} x_i(T) = \int_{T_i}^{T} v_i(t) \cos \theta_i(t) dt \\ y_i(T) = \int_{T_i}^{T} v_i(t) \sin \theta_i(t) dt \\ \theta_i(T) = \int_{T_i}^{T} v_i(t) \kappa_i(t) dt \\ v_i(T) = \int_{T_i}^{T} a_i(t) dt \end{bmatrix}, \quad \forall S_i = 1 \tag{20}$$

Step 3: Judge the condition the newly arriving vehicle meets. The aforementioned three conditions can be judged by Eq. (21)

$$c_i = \begin{cases} 1, & N = 0 \\ 2, & N \neq 0, \ N_{(3-M_i)} = 0 \\ 3, & \text{others} \end{cases} \tag{21}$$
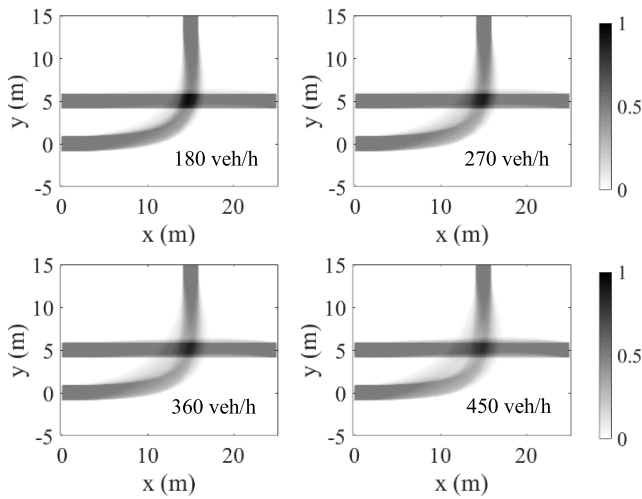
(a) FPC under different traffic volumes
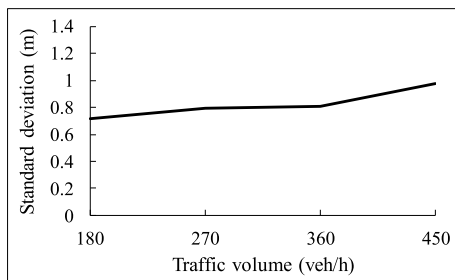


(b) Change of SD against the traffic volume

Fig. 9. Impact of the traffic volume.

where, $c_i$ is the condition the newly arriving vehicle $i$ encounters.

Step 4: Plan trajectories. The trajectory of the newly arriving vehicle and trajectories of vehicles with temporary trajectories can be planned or re-planned according to Eqs. (3) – (14) based on the Minimum Principle of Pontryagin [64], [66], [67].

Step 5: Update the fixed and temporary trajectories. Under conditions 1 and 2, only the trajectory of the newly arriving vehicle is planned. Then, the newly arriving vehicle gets the temporary trajectory. Under condition 3, the trajectories of the newly arriving vehicle and vehicles with temporary trajectories are planned. The vehicle crossing the conflict point first is given the fixed trajectory. Others get temporary trajectories.

Step 6: Stopping criteria. The iteration will be stopped if the time step reaches the end of the analysis period ($T_{end}$), and output the trajectories of all the vehicles. Otherwise, return to step 1. According to the trajectories, the path dispersion can be estimated.

Our modelling principle is parsimonious. The complex condition can be reflected by properly setting the proposed model's input parameters. (1) The impacts of the intersection type on the vehicular path mainly depend on the vehicle's heading angles on approach and exit lanes, while the impacts of the intersection size mainly lie in the positions of the approach and exit lanes. These reality factors related to the geometric layout can be reflected by the initial (the plane coordinate, the heading angle, and the velocity) and terminal states (the plane coordinate and the heading angle) of vehicles. (2) For various vehicle types, the impact on the vehicular path mainly depends on vehicle performance and driver's path preference. These factors relating to the vehicle can be reflected by the vehicle performance parameters (maximum velocity, minimum turning radius, and minimum and maximum acceleration) and driving behaviour parameters ($\beta_1$, $\beta_2$, $\beta_3$, and $\beta_4$). (3) For various traffic conditions, such as the traffic volume, the proportion of turning movements, and the vehicle type ratio, can be reflected by the setting of the vehicle generation rate for each movement and each vehicle type.

Please note that the optimal control theory is used to establish the simulation model. Its advantage lies in the interpretability of the vehicle trajectory. By setting the acceleration and curvature as control variables, we assume human drivers are optimal controllers to control the steering wheel and the brake/throttle pedals to minimize future costs. We used optimal control to model human driver behaviour. By keeping the model close to a natural form of control, the model can reproduce human behaviour in previously unseen cases. This is verified with the validation of the model on the intersections outside the test set in the next section.

## V. MODEL VALIDATION

This section validates the proposed model's descriptive power and accuracy using empirical data. The overall path dispersion of movements instead of a specific vehicular trajectory is compared between the simulation results and empirical data. Besides the five intersections used for parameter calibration, four new intersections (i.e., not being used in the calibration, No. 6 − 9 in Table I) are added to validate the proposed model's performance when the distribution of model parameters is unknown. They include a four-leg intersection, two T-shaped intersections and a Y-shaped intersection. We only explore the conflict movement pair between the unprotected left-turn and opposing through movements at intersections. Moreover, movements whose volumes are too small (smaller than 1 veh/min) are also removed to support the analysis. The validation methodology and results of the validation are presented as follows, in which the simulation results are the average values of 10 runs in each tested case. For comparison, we also compared the proposed model with a social force-based simulation model proposed by Ma [48].

The FPC results of four data sources/models are illustrated in Fig. 6, including (1) empirical data, (2) proposed model, (3) Ma's model, and (4) Vissim simulation (using the movement pair of westbound left-turn and eastbound through movement at intersection No. 8 as an example, see Table IV in Appendix A for the 12 pairs). We can find that the path dispersions of the empirical data and proposed model are visually comparable.

The comparison results of the paired-samples T-test (see Table V in Appendix A) show that there is no significant difference between the simulation result and empirical data ($p > 0.05$) under the meter-level FPC analysis. Ma's model can also reflect the path dispersions. However, the accuracy of the description is lower than that of the proposed model. The paired-samples T-test shows that 3 of 12 pairs (pairs 5, 9,

TABLE IV
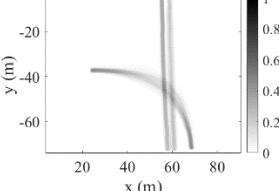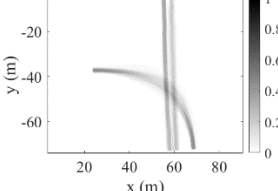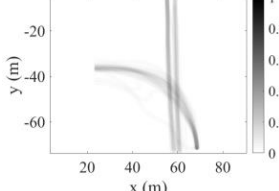FPC of the Empirical Data and Simulation Result
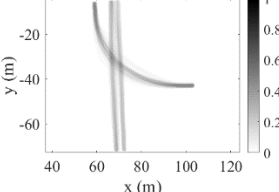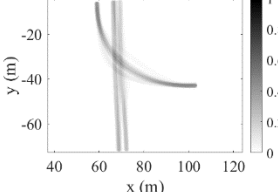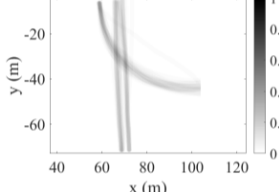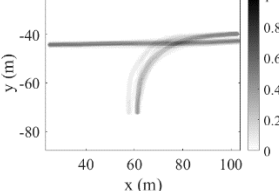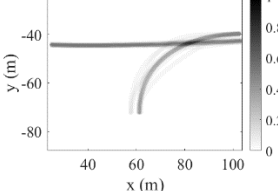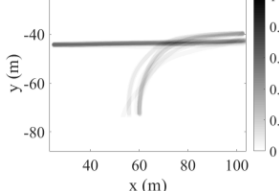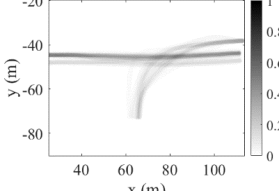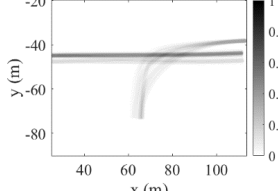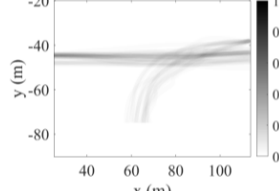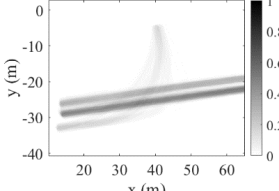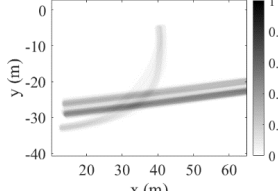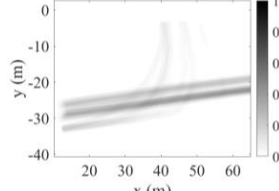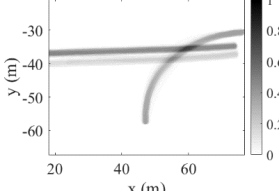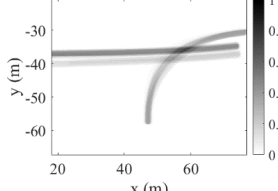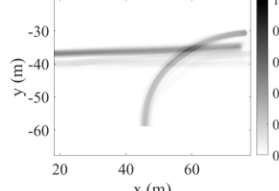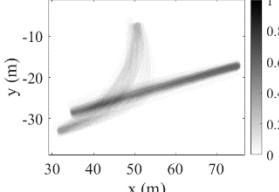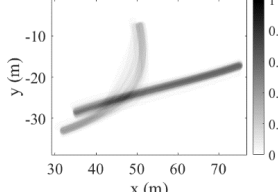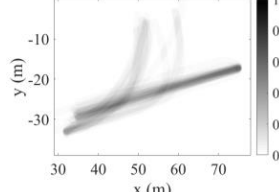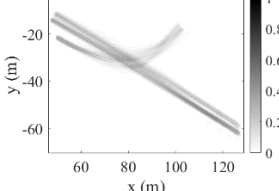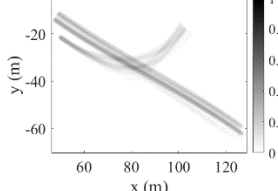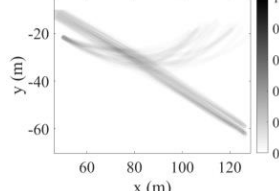
| Pair | Intersections | Movements | FPC of empirical trajectories | FPC of proposed model | FPC of Ma's model |
|------|---------------|-----------|-------------------------------|-----------------------|-------------------|
| Pair 1 | No. 1: Yangtai Road - Zhentai Road | NB LT – SB TH | | | |
| Pair 2 | No. 1: Yangtai Road - Zhentai Road | SB LT – NB TH | | | |
| Pair 3 | No. 1: Yangtai Road - Zhentai Road | WB LT – EB TH | | | |
| Pair 4 | No. 2: Youyi Road – Tieli Road | WB LT – EB TH | | | |
| Pair 5 | No. 3: Cangyi Road – Yuansheng Road | EB LT – WB TH | | | |
| Pair 6 | No. 4: Zuchongzhi Road – Gaosi Road | WB LT – EB TH | | | |
| Pair 7 | No. 5: Taolin Road – Linshan Road | EB LT – WB TH | | | |
| Pair 8 | No. 6: Gaokezhong Road - Zhangdong Road | EB LT – WB TH | | | |

This article has been accepted for inclusion in a future issue of this journal. Content is final as presented, with the exception of pagination.

ZHAO et al.: UNPROTECTED LEFT-TURN BEHAVIOR MODEL CAPTURING PATH VARIATIONS AT INTERSECTIONS 11

TABLE IV
*(Continued.)* FPC of the Empirical Data and Simulation Result



| Pair 9 | No. 6: Gaokezhong Road - Zhangdong Road | WB LT – EB TH | | | |
| Pair 10 | No. 7: Pingdu Road - Jinyang Road | WB LT – EB TH | | | |
| Pair 11 | No. 8: Tangxing Road - Tangzhen Road | WB LT – EB TH | | | |
| Pair 12 | No. 9: Jiaodong Road - Mouping Road | EB LT – WB TH | | | |
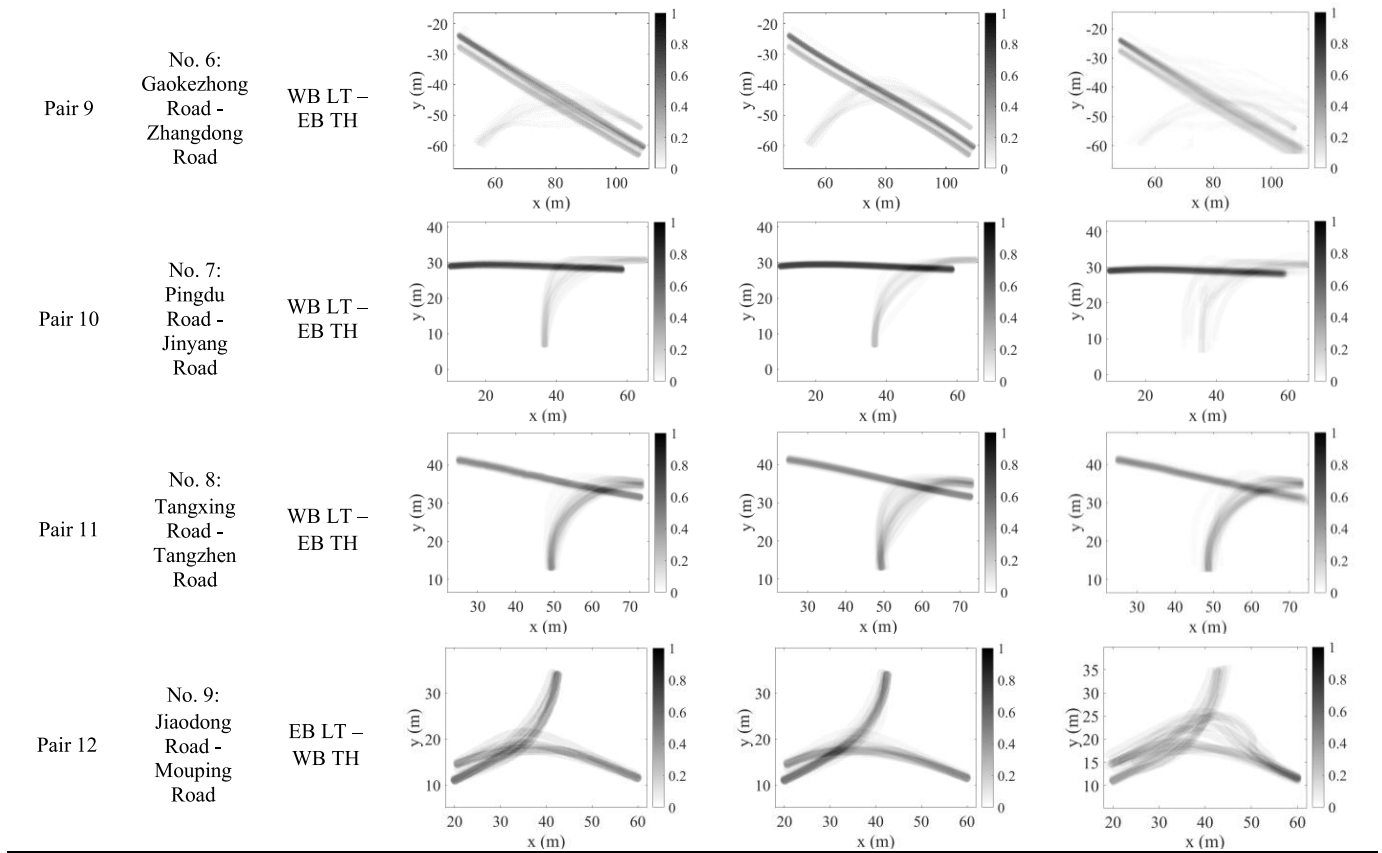
Note: EB, SB, WB, and NB indict eastbound, southbound, westbound, and northbound, respectively; LT and TH indict left-turn and through movement, respectively.

and 12) significantly differ between the simulation result and empirical data. The Vissim simulation results in all vehicles passing along the same path, and there is no path dispersion.

The proposed model also performs well in SD analysis (see Appendix B). Comparing the SD values between the simulation result of the proposed model and empirical data, the minimum, maximum, and average relative errors are 0.15%, 16.93%, and 8.55%, respectively. The significance test of the difference (paired-samples T-test) shows that the difference in SD between the two is not significant ($p > 0.05$). The validation does not show a significantly different performance than the calibration. Moreover, the validation shows that the model produces results of sufficient quality to represent the overall path dispersion of the left-turn and through movement interactions. This indicates that the model is applicable to practical problems. For Ma's model, the minimum, maximum, and average relative errors of the SD values are 14.52%, 207.36%, and 104.66%, respectively, which are much higher than those of the proposed model. The difference in SD between the simulation result of Ma's model and the empirical data is significant ($p < 0.05$). We also find that the SD values of Ma's model are larger than those of the empirical data and proposed model in all the tested cases. It may be because the trajectories of Ma's model are not directly obtained by driver

manoeuvres. The comparison shows that the proposed model outperforms Ma's model in capturing path variations in tested cases.

In turn, the simulation results of the proposed model can be used to assess designs. For intersection No. 8, the potential conflicting area is shown as the blue box in Fig. 6(b). The variability of the conflicting point location is high, which compromises traffic safety. Therefore, the guidance measures, such as guideline markings, stop and yield lines, channelizing islands, reflective road studs, and various guide signs, can be used to standardize the path of the left-turn traffic flow.

## VI. Application: Effects of Road Layouts and Traffic Conditions

Based on the proposed model, we explore the effect of the road layouts and traffic conditions on the path dispersion of the left-turn and through movement. The basic inputs of the numerical experiment are as follows. There are two conflicting movements: eastbound left-turn and westbound through movement. The left-turn moves from (0, 0) m to (20, 20) m. The initial heading angle, initial velocity, and terminal heading angle of left-turn are 0 rad, 8 m/s, and $\pi/2$ rad, respectively. The through movement moves from (37.5, 7.5) m to (0, 7.5) m. The initial heading angle, initial velocity, and

TABLE V
SIGNIFICANCE TEST OF THE DIFFERENCE IN FPC

| Pair | Proposed model | | | | | Sig. (2-tailed) | Ma's model | | | | | Sig. (2-tailed) |
|------|------|------|------|------|------|------|------|------|------|------|------|------|
| | Paired Differences | | | | | | Paired Differences | | | | | |
| | Mean | Std. deviation | Std. error mean | 95% Confidence interval of the difference | | | Mean | Std. deviation | Std. error mean | 95% Confidence interval of the difference | | |
| | | | | Lower | Upper | | | | | Lower | Upper | |
| 1 | 0.00034 | 0.02855 | 0.00050 | -0.00063 | 0.00131 | 0.490 | 0.00085 | 0.03250 | 0.00056 | -0.00025 | 0.00196 | 0.130 |
| 2 | -0.00047 | 0.06776 | 0.00125 | -0.00293 | 0.00199 | 0.706 | 0.00066 | 0.03596 | 0.00063 | -0.00058 | 0.00190 | 0.298 |
| 3 | 0.00031 | 0.02535 | 0.00045 | -0.00056 | 0.00118 | 0.489 | -0.00057 | 0.04316 | 0.00080 | -0.00214 | 0.00099 | 0.472 |
| 4 | 0.00116 | 0.04048 | 0.00060 | -0.00002 | 0.00233 | 0.054 | 0.00037 | 0.03505 | 0.00052 | -0.00065 | 0.00139 | 0.478 |
| 5 | 0.00049 | 0.05179 | 0.00098 | -0.00143 | 0.00240 | 0.617 | 0.00382 | 0.02698 | 0.00051 | 0.00282 | 0.00481 | 0.000 |
| 6 | 0.00057 | 0.03714 | 0.00078 | -0.00096 | 0.00210 | 0.464 | 0.00109 | 0.04121 | 0.00097 | -0.00082 | 0.00299 | 0.262 |
| 7 | 0.00165 | 0.03397 | 0.00090 | -0.00010 | 0.00341 | 0.065 | -0.00107 | 0.03129 | 0.00072 | -0.00248 | 0.00033 | 0.135 |
| 8 | 0.00070 | 0.04045 | 0.00060 | -0.00047 | 0.00188 | 0.241 | -0.00050 | 0.03840 | 0.00057 | -0.00161 | 0.00061 | 0.380 |
| 9 | 0.00095 | 0.04410 | 0.00081 | -0.00063 | 0.00253 | 0.239 | 0.00194 | 0.03285 | 0.00060 | 0.00076 | 0.00311 | 0.001 |
| 10 | -0.00079 | 0.03004 | 0.00078 | -0.00232 | 0.00074 | 0.312 | -0.00079 | 0.02814 | 0.00069 | -0.00215 | 0.00057 | 0.255 |
| 11 | -0.00091 | 0.05222 | 0.00126 | -0.00337 | 0.00155 | 0.468 | -0.00028 | 0.03052 | 0.00073 | -0.00172 | 0.00116 | 0.700 |
| 12 | 0.00116 | 0.05573 | 0.00157 | -0.00192 | 0.00424 | 0.460 | -0.00397 | 0.07001 | 0.00197 | -0.00784 | -0.00010 | 0.044 |

terminal heading angle for through movement are $-\pi$ rad, 8 m/s, and $-\pi$ rad, respectively. The traffic volumes for both movements are 360 veh/h. For each case, the simulation time is one hour.

### A. Impact of the Intersection's Spatial Size

Drivers have more path options when the spatial size of the intersection increases. The intersection spatial size is changed from 0.5 to 2 times the basic input size to explore its effect on the path dispersion. The FPC under each intersection size and changes in the SD are shown in Fig. 7. Fig. 7(a) shows that path dispersion becomes increasingly discrete with increasing intersection spatial size. The changes in the SD shown in Fig. 7(b) also illustrate this. It is because when the intersection spatial size is small, drivers do not have many options to choose from due to the turning radius limit (5 m in this experiment). With the increase in the intersection spatial size, the trajectory is not restricted too much by the minimum turning radius. Drivers can choose to pre-empt the conflict point with a sharp turning or yield with smooth turning.

### B. Impact of the Crossing Angle

A large crossing angle may cause left-turn difficulties. The crossing angle is changed from $\pi/4$ to $3\pi/4$ at $\pi/8$ intervals to explore its effect on the path dispersion. The changes in FPC and SD against the crossing angle are shown in Fig. 8. The results show that with the increase of the crossing angle, the path distribution is less dispersive. It is also related to possible options. When the crossing angle is small, the left-turn vehicles do not need to turn too much indicating that there are multiple possibilities. Fig. 8(a) shows two classes of paths when the crossing angle is small. One is a direct turning path, while another is a detour turning where drivers try to avoid the conflict while saving time. However, when the crossing angle is large, this phenomenon is not observed because there is no detour option for a limited space and turning radius.

### C. Impact of the Traffic Volume

High traffic volume increases the probability of conflict, which may make the traffic condition more complex. The traffic volume is changed from 180 veh/h to 450 veh/h at 90 veh/h intervals to explore its effect on the path dispersion. The FPC under each case and the changes in the SD are shown in Fig. 9. The SD values increase with the increase in traffic volume. Drivers can encounter more conflicts under high traffic volumes, which increases path dispersion. However, the changes are slight compared to changes in the intersection spatial size and the crossing angle analysis. The difference in FPC is also not visually significant.

## VII. CONCLUSION

This study explored the *overall* path dispersion of unprotected left-turn and opposing through movement at intersections. A simulation model considering the behaviour of drivers was established, and the parameters were calibrated. The proposed model was validated using empirical data, demonstrating the effectiveness of the model in describing and qualitatively analysing the path dispersion. The effects of road layouts and traffic conditions on the path dispersion of left-turn and through movement were discussed based on sensitivity analysis. The following findings are drawn from the study:

(1) The simulation model describes the overall path dispersion by generating both tactical decisions and operational trajectories in a single mathematical framework. The proposed simulation model can endogenously describe the paths of interacting vehicles by planning 2D trajectories based on optimal control It solves the problem of state-of-the-art simulation tools in which the paths of interacting vehicles were set as inputs for simulating 1D traffic flow.

(2) The proposed simulation model performs well for both the calibrated intersections and newly added intersections without model parameter recalibration. This is achieved by

randomly selecting parameters from the calibrated ranges for individual vehicles. The model can represent the path dispersion of left-turn and opposing through movement with an average error of 8.92%.

(3) The path dispersion of the left-turn and through movement increases with the growth of the intersection spatial size and traffic volume, while decreasing with the growth of the crossing angle. Compared with the traffic condition (traffic volume), the road layouts (intersection spatial size and crossing angle) have a more significant effect on path dispersion.

In practice, modelling the path dispersion at intersections can help engineers recommend the design of intersections configuration and management. For example, the result is drawn from the sensitivity analysis of the model that the degree of the path dispersion is restricted by the possible trajectories the drivers can choose. Under stronger space and turning radius constraints, e.g., small intersections, the traffic flow operates more orderly than in larger intersections. It can verify the predictive power and rationality of the model because the result is consistent with intuition. The sensitivity analysis result indicates the direction to normalise the vehicle path inside the intersection. Different methods, such as traffic channelisation, traffic islands, and radius design of curbs, can be used to strengthen the constraint on the vehicle path. Our simulation model provides a scientifically sound and empirically underpinned tool to evaluate intersection design alternatives, and can be used to determine where to place these traffic management facilities.

This study is the first step to exploring the overall path dispersion, which has the potential to explain chaos at intersections. The direction of future studies can be the analysis of the effects of the complex geometric, traffic, and control conditions on the path dispersion based on more empirical data. These studies will lead to the design of new measures to guide drivers to cross the intersection orderly, which is valuable for the meticulous geometric design and traffic management of intersections. For the connection of the discrete paths inside the intersection and the paths on the road segments, we think there are two ways to deal with the problem in the next step. One way (a simple and convenient way) is to fix the start and end points of the movements inside intersections, such as the middle of each approach and exit traffic lanes. Then we can simulate the microscopic traffic flow at segments and intersections using the existing tools and the proposed model, respectively. Another way (a more complex way) is that the 2D trajectory planning model can also describe the microscopic traffic flow at segments by extending the proposed model considering the constraints caused by lane markings. Then we can simulate the microscopic traffic flow at segments and intersections using a unified 2D trajectory planning model.

## APPENDIX A
## COMPARISON OF THE DIFFERENCE IN FPC

The FPC of the empirical data and simulation results are shown in Table IV. The paired-sample T-test of FPCs between the simulation result and empirical data is shown in Table V.

### TABLE VI
### COMPARISON OF SD BETWEEN EMPIRICAL DATA AND SIMULATION RESULTS

| Pair | SD of empirical trajectories | Proposed model | | Ma's model | |
|---|---|---|---|---|---|
| | | SD | Relative error | SD | Relative error |
| Pair 1 | 1.323 | 1.184 | 10.53% | 3.491 | 163.87% |
| Pair 2 | 1.162 | 1.163 | 0.15% | 3.128 | 169.19% |
| Pair 3 | 1.289 | 1.385 | 7.47% | 1.535 | 19.08% |
| Pair 4 | 1.893 | 1.763 | 6.88% | 2.678 | 41.47% |
| Pair 5 | 1.114 | 1.055 | 5.31% | 3.424 | 207.36% |
| Pair 6 | 0.567 | 0.641 | 13.00% | 1.209 | 113.23% |
| Pair 7 | 1.328 | 1.103 | 16.93% | 3.083 | 132.15% |
| Pair 8 | 1.421 | 1.502 | 5.70% | 2.951 | 107.67% |
| Pair 9 | 1.177 | 1.346 | 14.35% | 3.201 | 171.96% |
| Pair 10 | 1.209 | 1.258 | 4.05% | 2.204 | 82.30% |
| Pair 11 | 1.563 | 1.376 | 11.95% | 1.790 | 14.52% |
| Pair 12 | 0.909 | 0.851 | 6.32% | 1.210 | 33.11% |
| Average | | | 8.55% | | 104.66% |

### TABLE VII
### SIGNIFICANCE TEST OF THE DIFFERENCE IN SD

| Model | Mean | Std. Deviation | Std. Error Mean | 95% Confidence Interval of the Difference | | Sig. (2-tailed) |
|---|---|---|---|---|---|---|
| | | | | Lower | Upper | |
| Proposed model | 0.027 | 0.125 | 0.036 | -0.052 | 0.107 | 0.465 |
| Ma's model | -1.246 | 0.799 | 0.231 | -1.753 | -0.738 | 0.000 |

## APPENDIX B
## COMPARISON OF THE DIFFERENCE IN SD VALUES

The comparison of the SD values between the simulation result and empirical data is shown in Table VI. The significance test of the difference in SD is shown in Table VII.

## REFERENCES

[1] A. Zgonnikov, D. Abbink, and G. Markkula, "Should I stay or should I go? Cognitive modeling of left-turn gap acceptance decisions in human drivers," *Hum. Factors*, 2022, doi: 10.1177/00187208221144561.

[2] H. Zhu, S. Zhu, M. Iryo-Asano, and H. Nakamura, "Investigating driver reactions to movements of autonomous vehicle in permitted right turn through driving simulator experiments," *Transp. Res. F, Traffic Psychol. Behaviour*, vol. 89, pp. 385–398, Aug. 2022.

[3] C. Chai and Y. D. Wong, "Fuzzy cellular automata model for signalized intersections," *Comput.-Aided Civil Infrastruct. Eng.*, vol. 30, no. 12, pp. 951–964, Dec. 2015.

[4] T.-Q. Tang, X.-F. Luo, J. Zhang, and L. Chen, "Modeling electric bicycle's lane-changing and retrograde behaviors," *Phys. A, Stat. Mech. Appl.*, vol. 490, pp. 1377–1386, Jan. 2018.

[5] Y. Gao, Y. Liu, H. Hu, and Y. E. Ge, "Intersection dilemma-zone protection as a dynamic signal-optimization problem with model predictive control," *J. Transp. Eng., A, Syst.*, vol. 145, no. 11, Nov. 2019, Art. no. 04019046.

[6] Y. Sun, B. Xie, and D. Wu, "Three methods of PCU estimation at signalized intersections under mixed traffic with UAV monitoring data," *J. Transp. Eng., A, Syst.*, vol. 148, no. 3, Mar. 2022, Art. no. 04021118.

[7] R. K. Padinjarapat and T. V. Mathew, "Estimation of saturation flow for non-lane based mixed traffic streams," *Transportmetrica B, Transp. Dyn.*, vol. 9, no. 1, pp. 42–61, Jan. 2021.

[8] Y. Wei, K. Li, and K. Tang, "Trajectory-based identification of critical instantaneous decision events at mixed-flow signalized intersections," *Accident Anal. Prevention*, vol. 123, pp. 324–335, Feb. 2019.

[9] R. Chauhan, A. Dhamaniya, and S. Arkatkar, "Spatiotemporal variation of rear-end conflicts at signalized intersections under disordered traffic conditions," *J. Transp. Eng., A, Syst.*, vol. 147, no. 11, Nov. 2021, Art. no. 05021007.

[10] X. Yan and E. Radwan, "Effect of restricted sight distances on driver behaviors during unprotected left-turn phase at signalized intersections," *Transp. Res. F, Traffic Psychol. Behaviour*, vol. 10, no. 4, pp. 330–344, Jul. 2007.

[11] P. C. Devarasetty, Y. Zhang, and K. Fitzpatrick, "Differentiating between left-turn gap and lag acceptance at unsignalized intersections as a function of the site characteristics," *J. Transp. Eng.*, vol. 138, no. 5, pp. 580–588, May 2012.

[12] M. Liu, G. Lu, Y. Wang, and Z. Zhang, "Analyzing drivers' crossing decisions at unsignalized intersections in China," *Transp. Res. F, Traffic Psychol. Behav.*, vol. 24, pp. 244–255, May 2014.

[13] M. Liu, G. Lu, Y. Wang, Y. Wang, and Z. Zhang, "Preempt or yield? An analysis of driver's dynamic decision making at unsignalized intersections by classification tree," *Saf. Sci.*, vol. 65, pp. 36–44, Jun. 2014.

[14] G. R. Patil and D. S. Pawar, "Temporal and spatial gap acceptance for minor road at uncontrolled intersections in India," *Transp. Res. Rec., J. Transp. Res. Board*, vol. 2461, no. 1, pp. 129–136, Jan. 2014.

[15] J. M. Hutton, K. M. Bauer, C. A. Fees, and A. Smiley, "Evaluation of left-turn lane offset using the naturalistic driving study data," *J. Saf. Res.*, vol. 54, pp. 1–5, Sep. 2015.

[16] C. J. Robbins, H. A. Allen, and P. Chapman, "Comparing drivers' gap acceptance for cars and motorcycles at junctions using an adaptive staircase methodology," *Transp. Res. F, Traffic Psychol. Behaviour*, vol. 58, pp. 944–954, Oct. 2018.

[17] X. Yan, E. Radwan, and D. Guo, "Effects of major-road vehicle speed and driver age and gender on left-turn gap acceptance," *Accident Anal. Prevention*, vol. 39, no. 4, pp. 843–852, Jul. 2007.

[18] J. Bärgman, K. Smith, and J. Werneke, "Quantifying drivers' comfort-zone and dread-zone boundaries in left turn across path/opposite direction (LTAP/OD) scenarios," *Transp. Res. F, Traffic Psychol. Behaviour*, vol. 35, pp. 170–184, Nov. 2015.

[19] K. Tang, D. Di, and K. Li, "Risk-taking behavior of left-turners in gap acceptance and its effects on capacity estimation at signalized intersections," *Transp. Res. Rec., J. Transp. Res. Board*, vol. 2483, no. 1, pp. 1–9, Jan. 2015.

[20] M. Liu, Y. Chen, G. Lu, and Y. Wang, "Modeling crossing behavior of drivers at unsignalized intersections with consideration of risk perception," *Transp. Res. F, Traffic Psychol. Behaviour*, vol. 45, pp. 14–26, Feb. 2017.

[21] Y. Mao et al., "A measurement to driving situation awareness in signalized intersections," *Transp. Res. D, Transp. Environ.*, vol. 62, pp. 739–747, Jul. 2018.

[22] E. Paschalidis, C. F. Choudhury, and S. Hess, "Modelling the effects of stress on gap-acceptance decisions combining data from driving simulator and physiological sensors," *Transp. Res. F, Traffic Psychol. Behaviour*, vol. 59, pp. 418–435, Nov. 2018.

[23] Y. Gao, Y. Liu, H. Hu, and Y.-E. Ge, "Modeling traffic operation at signalized intersections without explicit left-turn yielding rules with an enhanced cell transmission model," *J. Adv. Transp.*, vol. 50, no. 7, pp. 1470–1488, Nov. 2016.

[24] Y. Gao, Y. Liu, H. Hu, and Y. E. Ge, "Signal optimization for an isolated intersection with illegal permissive left-turning movement," *Transportmetrica B, Transp. Dyn.*, vol. 7, no. 1, pp. 928–949, Dec. 2019.

[25] X. Li, O. Oviedo-Trespalacios, and A. Rakotonirainy, "Drivers' gap acceptance behaviours at intersections: A driving simulator study to understand the impact of mobile phone visual-manual interactions," *Accident Anal. Prevention*, vol. 138, Apr. 2020, Art. no. 105486.

[26] M. Mohan and S. Chandra, "Critical gap estimation at two-way stop-controlled intersections based on occupancy time data," *Transportmetrica A, Transp. Sci.*, vol. 14, no. 4, pp. 316–329, Apr. 2018.

[27] G. F. Newell, "A simplified car-following theory: A lower order model," *Transp. Res. B, Methodol.*, vol. 36, no. 3, pp. 195–205, 2002.

[28] S. Ahn, M. J. Cassidy, and J. A. Laval, "Verification of a simplified car-following theory," *Transp. Res. B, Methodol.*, vol. 38, no. 5, pp. 431–440, 2004.

[29] M. Sasaki and T. Nagatani, "Transition and saturation of traffic flow controlled by traffic lights," *Phys. A, Stat. Mech. Appl.*, vol. 325, nos. 3–4, pp. 531–546, Jul. 2003.

[30] T. Tang et al., "A traffic flow model considering signal light influence and its numerical simulation," *Acta Phys. Sinica*, vol. 57, no. 1, pp. 56–60, 2008.

[31] S. Yu and Z. Shi, "Analysis of car-following behaviors considering the green signal countdown device," *Nonlinear Dyn.*, vol. 82, nos. 1–2, pp. 731–740, Oct. 2015.

[32] T. Tang, Z. Yi, J. Zhang, and N. Zheng, "Modelling the driving behaviour at a signalised intersection with the information of remaining green time," *IET Intell. Transp. Syst.*, vol. 11, no. 9, pp. 596–603, Nov. 2017.

[33] M. Saifuzzaman and Z. Zheng, "Incorporating human-factors in car-following models: A review of recent developments and research needs," *Transp. Res. C, Emerg. Technol.*, vol. 48, pp. 379–403, Nov. 2014.

[34] J. Zhao and P. Li, "An extended car-following model with consideration of speed guidance at intersections," *Phys. A, Stat. Mech. Appl.*, vol. 461, pp. 1–8, Nov. 2016.

[35] T.-Q. Tang, J. Zhang, and K. Liu, "A speed guidance model accounting for the driver's bounded rationality at a signalized intersection," *Phys. A, Stat. Mech. Appl.*, vol. 473, pp. 45–52, May 2017.

[36] R. Hoogendoorn, B. van Arerm, and S. Hoogendoom, "Automated driving, traffic flow efficiency, and human factors: Literature review," *Transp. Res. Rec., J. Transp. Res. Board*, vol. 2422, no. 1, pp. 113–120, Jan. 2014.

[37] Y. Li, C. Tang, S. Peeta, and Y. Wang, "Nonlinear consensus-based connected vehicle platoon control incorporating car-following interactions and heterogeneous time delays," *IEEE Trans. Intell. Transp. Syst.*, vol. 20, no. 6, pp. 2209–2219, Jun. 2019.

[38] Y. Li, W. Chen, S. Peeta, and Y. Wang, "Platoon control of connected multi-vehicle systems under V2X communications: Design and experiments," *IEEE Trans. Intell. Transp. Syst.*, vol. 21, no. 5, pp. 1891–1902, May 2020.

[39] B. Gunay, "Car following theory with lateral discomfort," *Transp. Res. B, Methodol.*, vol. 41, no. 7, pp. 722–735, Aug. 2007.

[40] S. Jin, D. Wang, P. Tao, and P. Li, "Non-lane-based full velocity difference car following model," *Phys. A, Stat. Mech. Appl.*, vol. 389, no. 21, pp. 4654–4662, Nov. 2010.

[41] V. Kanagaraj and M. Treiber, "Self-driven particle model for mixed traffic and other disordered flows," *Phys. A, Stat. Mech. Appl.*, vol. 509, pp. 1–11, Nov. 2018.

[42] R. Delpiano, J. C. Herrera, J. Laval, and J. E. Coeymans, "A two-dimensional car-following model for two-dimensional traffic flow problems," *Transp. Res. C, Emerg. Technol.*, vol. 114, pp. 504–516, May 2020.

[43] D.-F. Xie, Z.-Y. Gao, X.-M. Zhao, and K.-P. Li, "Characteristics of mixed traffic flow with non-motorized vehicles and motorized vehicles at an unsignalized intersection," *Phys. A, Stat. Mech. Appl.*, vol. 388, no. 10, pp. 2041–2050, May 2009.

[44] G. Zhang, Y. Qi, and J. Chen, "Exploring factors impacting paths of left-turning vehicles from minor road approach at unsignalized intersections," *Math. Problems Eng.*, vol. 2016, pp. 1–9, Jan. 2016.

[45] M. N. Azadani and A. Boukerche, "A novel multimodal vehicle path prediction method based on temporal convolutional networks," *IEEE Trans. Intell. Transp. Syst.*, vol. 23, no. 12, pp. 25384–25395, Dec. 2022.

[46] J. Choi, R. Tay, S. Kim, and S. Jeong, "Turning movements, vehicle offsets and ageing drivers driving behaviour at channelized and unchannelized intersections," *Accident Anal. Prevention*, vol. 108, pp. 227–233, Nov. 2017.

[47] T. Zhang, W. Song, M. Fu, Y. Yang, and M. Wang, "Vehicle motion prediction at intersections based on the turning intention and prior trajectories model," *IEEE/CAA J. Autom. Sinica*, vol. 8, no. 10, pp. 1657–1666, Oct. 2021.

[48] Z. Ma, J. Xie, X. Qi, Y. Xu, and J. Sun, "Two-dimensional simulation of turning behavior in potential conflict area of mixed-flow intersections," *Comput.-Aided Civil Infrastruct. Eng.*, vol. 32, no. 5, pp. 412–428, May 2017.

[49] M. Fellendorf, R. Schonauer, and W. Huang, "Social force based vehicle model for two-dimensional spaces," in *Proc. Transp. Res. Board 91st Annu. Meeting*, Washington, DC, USA, 2012, pp. 12–1347.

[50] D. Yang, X. Zhou, G. Su, and S. Liu, "Model and simulation of the heterogeneous traffic flow of the urban signalized intersection with an island work zone," *IEEE Trans. Intell. Transp. Syst.*, vol. 20, no. 5, pp. 1719–1727, May 2019.

[51] D. N. Huynh, M. Boltze, and A. T. Vu, "Modelling mixed traffic flow at signalized intersectionusing modified social force model," *J. Eastern Asia Soc. Transp. Stud.*, vol. 10, pp. 1734–1749, Dec. 2013.

This article has been accepted for inclusion in a future issue of this journal. Content is final as presented, with the exception of pagination.

ZHAO et al.: UNPROTECTED LEFT-TURN BEHAVIOR MODEL CAPTURING PATH VARIATIONS AT INTERSECTIONS 15

[52] Z. Ma, J. Sun, and Y. Wang, "A two-dimensional simulation model for modelling turning vehicles at mixed-flow intersections," *Transp. Res. C, Emerg. Technol.*, vol. 75, pp. 103–119, Feb. 2017.

[53] W. K. M. Alhajyaseen, M. Asano, H. Nakamura, and D. M. Tan, "Stochastic approach for modeling the effects of intersection geometry on turning vehicle paths," *Transp. Res. C, Emerg. Technol.*, vol. 32, pp. 179–192, Jul. 2013.

[54] S. R. Bonela and B. R. Kadali, "Analysis of right-turn vehicular driving paths at uncontrolled T-intersections," *Int. J. Injury Control Saf. Promotion*, vol. 30, no. 1, pp. 91–105, Jan. 2023.

[55] M. Yang, H. Yu, and L. Bai, "Simulation-based evaluation of variation in left-turn paths in the coordinated intersection management," *J. Adv. Transp.*, vol. 2021, Dec. 2021, Art. no. 6243530.

[56] D. Gonzáleza, J. Pérezb, and V. Milanés, "Parametric-based path generation for automated vehicles at roundabouts," *Exp. Syst. Appl.*, vol. 71, pp. 332–341, Apr. 2017.

[57] Y. Bichiou and H. A. Rakha, "Developing an optimal intersection control system for automated connected vehicles," *IEEE Trans. Intell. Transp. Syst.*, vol. 20, no. 5, pp. 1908–1916, May 2019.

[58] Y. Bichiou and H. A. Rakha, "Real-time optimal intersection control system for automated/cooperative vehicles," *Int. J. Transp. Sci. Technol.*, vol. 8, no. 1, pp. 1–12, Mar. 2019.

[59] J. Zhao, V. L. Knoop, and M. Wang, "Two-dimensional vehicular movement modelling at intersections based on optimal control," *Transp. Res. B, Methodol.*, vol. 138, pp. 1–22, Aug. 2020.

[60] C. Dias, M. Iryo-Asano, M. Abdullah, T. Oguchi, and W. Alhajyaseen, "Modeling trajectories and trajectory variation of turning vehicles at signalized intersections," *IEEE Access*, vol. 8, pp. 109821–109834, 2020.

[61] C. Ziegler, V. Willert, and J. Adamy, "Modeling driving behavior of human drivers for trajectory planning," *IEEE Trans. Intell. Transp. Syst.*, vol. 23, no. 11, pp. 20889–20898, Nov. 2022.

[62] *Specification for Design of Urban Road Engineering*, SURCTC, China Architecture & Building Press, Beijing, China, 2012.

[63] T.-Q. Tang, Z.-Y. Yi, J. Zhang, T. Wang, and J.-Q. Leng, "A speed guidance strategy for multiple signalized intersections based on car-following model," *Phys. A, Stat. Mech. Appl.*, vol. 496, pp. 399–409, Apr. 2018.

[64] M. Wang, W. Daamen, S. P. Hoogendoorn, and B. van Arem, "Rolling horizon control framework for driver assistance systems. Part I: Mathematical formulation and non-cooperative systems," *Transp. Res. C, Emerg. Technol.*, vol. 40, pp. 271–289, Mar. 2014.

[65] J. Nocedal and S. Wright, *Numerical Optimization*. Berlin, Germany: Springer, 2006.

[66] M. Wang, W. Daamen, S. P. Hoogendoorn, and B. van Arem, "Rolling horizon control framework for driver assistance systems. Part II: Cooperative sensing and cooperative control," *Transp. Res. C, Emerg. Technol.*, vol. 40, pp. 290–311, Mar. 2014.

[67] L. S. Pontryagin, *Mathematical Theory of Optimal Processes*. New York, NY, USA: CRC press, 1987.

**Victor L. Knoop** was born in The Netherlands in 1981. He received the M.S. degree in physics from Leiden University in 2005 and the Ph.D. degree from the Delft University of Technology in 2009 on the effects of incidents on driving behavior and traffic congestion.

He was a Post-Doctoral Researcher with the University of Lyon from 2009 to 2010 on lane changing. He worked with the Imperial College London and the University of California at Berkeley. Since 2018, he has been a tenured Associate Professorship with the Transport and Planning Department, Delft University of Technology. He is currently the Co-Director of the Traffic Dynamics Modelling and Control Laboratory (TDMaC-Lab). His main research interests include interaction between microscopic and macroscopic traffic flow phenomena.

**Jian Sun** received the Ph.D. degree in transportation engineering from Tongji University, Shanghai, China. He is currently a Professor in transportation engineering with Tongji University. His research interests include intelligent transportation systems, traffic flow theory, AI in transportation, and traffic simulation.

**Zian Ma** was born in Hebei, China, in 1991. He received the B.S. and Ph.D. degrees in traffic and transportation engineering from Tongji University, Shanghai, China, in 2014 and 2020, respectively. His research interests include driving behavior, traffic flow theory, traffic simulation, and traffic control and management.

**Meng Wang** (Member, IEEE) was born in China in 1980. He received the B.Sc. degree in civil engineering from Tsinghua University and the M.Sc. degree in transportation engineering from the Research Institute of Highway and the Ph.D. degree (Hons.) from the Delft University of Technology (TU Delft), The Netherlands, in 2006 and 2014, respectively.

He worked as a Researcher with the National ITS Engineering Centre, China, from 2006 to 2009. From 2014 to 2015, he worked as a Post-Doctoral Researcher with the Department of BioMechanical Engineering, TU Delft, where he worked as an Assistant Professor (tenured since 2019) with the Department of Transport and Planning, from 2015 to 2021. He was the Co-Director of the Research Laboratory on Electric and Automated Transport (hEAT Laboratory). Since 2021, he has been working as a Professor with the "Friedrich List" Faculty of Transport and Traffic Sciences, TU Dresden. He is currently the Head of the Chair of Traffic Control and Process Automation. His main research interests are decision-making and control design of cooperative driving systems and traffic flow impact assessment of such systems. He is an Associate Editor of IEEE TRANSACTIONS ON INTELLIGENT TRANSPORTATION SYSTEMS, *IET ITS*, and *Transportmetrica B*.

**Jing Zhao** was born in Shanghai, China, in 1983. He received the B.S., M.S., and Ph.D. degrees in traffic engineering from Tongji University, Shanghai, in 2006, 2009, and 2014, respectively.

From 2014 to 2016, he was an Assistant Professor with the Traffic Engineering Department, University of Shanghai for Science and Technology, Shanghai. From 2017 to 2020, he was an Associate Professor. Since 2021, he has been working as a Professor and the Director of the Department of Traffic Engineering, University of Shanghai for Science and Technology. He is the first author of more than 40 articles in SCI/SSCI indexed journals. His research interests include traffic control and management, traffic flow model, and transit systems.